Particle Accelerators
1976, Vol. 7, pp. 111–117

RESIDUAL RADIOACTIVITY IN THE FERMILAB ACCELERATOR ENCLOSURES

J. H. McCRARY and H. H. CASEBOLT, Jr.

Fermi National Accelerator Laboratory, Batavia, Illinois 60510, USA

(*Received February 3, 1976; in final form March 18, 1976*)

A self-propelled radiation survey vehicle is used to make periodic measurements of the radiation levels in the various Fermilab accelerator enclosures resulting from residual radioactivity induced by losses from the proton beam. The vehicle is equipped with instrumentation which provides a strip chart record of the radiation intensity as a function of position and the mean radiation intensity of a given segment of the accelerator. Plots of the mean radiation intensity as a function of time for the past year and a half are presented here for several of the accelerator enclosures.

INTRODUCTION

The residual radioactivity present in the Fermilab beam-line enclosures is induced by high-energy protons lost from the primary beam. These protons cause spallation reactions and nuclear cascades in the steel, copper, concrete, and other materials comprising the vacuum system, magnets, supporting structures, and enclosure walls of the accelerator. Virtually all isotopes lighter than the elements present in these materials can be formed through nuclear reactions initiated by the primary protons. Thus, the radiation in the accelerator enclosures consists of β- and γ-ray emissions from many radioactive isotopes. While the resulting radiation spectrum is complex and is a function of both time and position, its combined interaction with matter resembles that of 1-MeV γ-radiation. The pattern of build-up and decay of residual radioactivity as functions of position and time is important to: (1) both the short-term and long-term improvement of accelerator operating efficiency, (2) the consideration of proposed changes in modes of operation, and (3) the determination and prediction of safe working conditions within the accelerator enclosures.

Figure 1 is a schematic drawing (not to scale) showing the relative location of the several Fermilab accelerator enclosures. Arrows in the figure denote beam direction. 200-MeV protons are injected from the Linac into the Booster. From the Booster, 8-GeV protons are injected into the Main Ring where their energy is increased to 400 GeV. The Main Ring is divided into six equal sectors which are designated by the letters A through F. The upstream end of each of these sectors contains a 52-meter straight section which bears the additional designation of "zero." Thus, Main Ring injection and extraction take place in the Transfer Hall which is located at A-0. The beam abort target, located at D-0, is a series of beam stops located radially outward onto which a small fraction of the beam is dumped at the end of slow spill extraction. The 400-GeV protons are extracted from the Main Ring in the Transfer Hall and distributed to the three major experimental areas through the Switchyard which is comprised of Enclosures B, C, D, and E. (For a more detailed

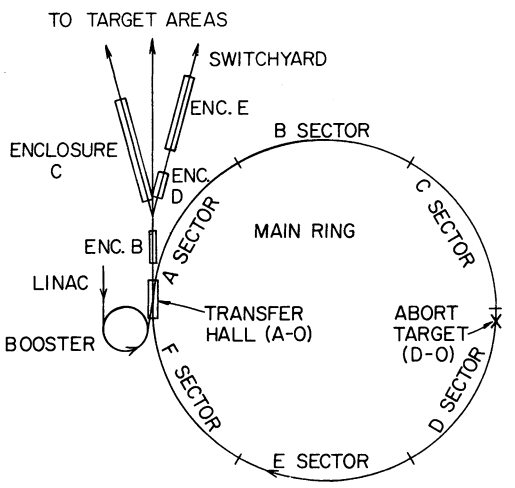

FIGURE 1 Schematic diagram of the Fermilab accelerator.

description of the Fermilab accelerator and its components, see Reference 1.)

To provide an indication of the scale of the accelerator system: the Linac length and the Booster diameter are both 150 meters; the Main Ring diameter is 2000 meters; Enclosure B is 130 meters long and Enclosure C is 330 meters long.

PROCEDURE

The Fermilab radiation survey vehicle is a modified battery-powered golf cart.[2] The cart is equipped with a Geiger–Mueller tube, a logarithmic count-rate meter, a strip chart recorder and a scaler. A permanent magnet attached to the rim of one of the wheels trips a magnetic switch as the wheel rotates. The signal thus obtained is used both to advance the strip chart and to gate on the scaler for a 50 msec time period. Over the speed range (0–15 km/h) of the golf cart the chart drive speed is directly proportional to the vehicle speed. One centimeter on the chart paper corresponds to 43 meters of vehicle travel. Although an effort is made to maintain a fixed distance of 30 cm between the G-M tube and the beam-line devices during the conduct of the survey, experience has shown that this parameter is not critical. The number of counts registered on the scaler from the G-M tube is, to a first approximation, independent of the vehicle speed, and is proportional to the radiation intensity averaged over a given length of enclosure. The approximation is good since the vehicle moves only 20 cm per counting period at its top speed. The equipment has been calibrated and the proportionality constants which relate total counts to mean radiation intensity have been determined for all segments of the various enclosures. Corrections for detector dead time are made to the observed count rates.

During normal accelerator operations, one day of each week is devoted to routine maintenance work which requires access to beam-line enclosures by work crews. Immediately prior to these accesses,

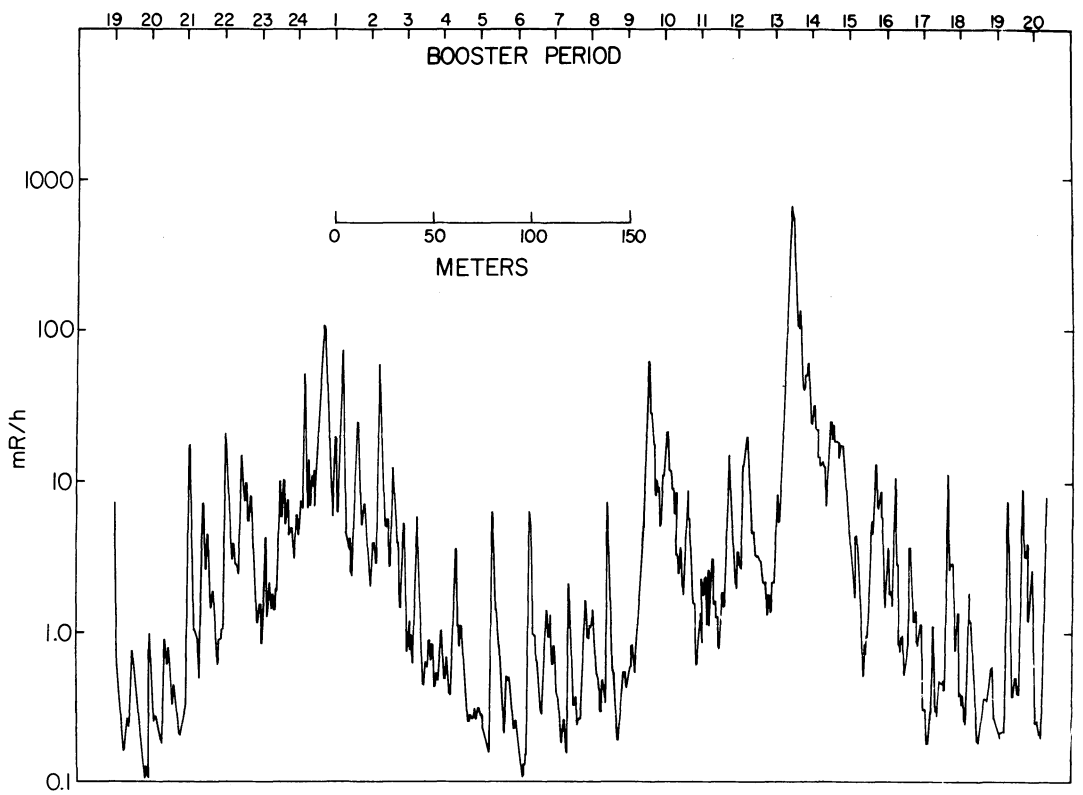

FIGURE 2 Radiation survey vehicle strip chart of the Fermilab Booster Accelerator showing a plot of radiation intensity vs position. The numbered marks at the top of the figure indicate the position of the short straight section in each Booster period. This survey was made on October 23, 1975.

radiation surveys are conducted in all of the enclosures in order to establish safe working conditions and maximum occupancy times. The enclosures in which the radiation survey vehicle is used include the 8-GeV Booster Accelerator, the 400-GeV Main Ring, and the Switchyard.

RESULTS

Figures 2, 3, and 4 are reproductions of strip charts obtained with the survey vehicle in the Booster, the Main Ring, and the Switchyard, respectively. It should be noted that due to the highly compressed distance scale on these strip charts, the extremely narrow peaks which appear as "fine structure" on the broader features are real and are reproducible.

The Booster chart shown in Figure 2 was made on October 23, 1975, $1\frac{1}{2}$ hours after the beam had been turned off. The important features on this graph are the injection (period 1) and extraction (period 13) regions of the accelerator. Also clearly visible in this plot are the increased levels of radioactivity present in all of the 24 short straight sections, located at the period markers. The Main Ring chart shown in Figure 3 was made on October 16, 1975, 24 hours after the beam had been turned off. The major loss points in the Main Ring are the Transfer Hall where both injection and extraction take place and the beam abort target located in D sector. A typical Switchyard chart is shown in Figure 4. This survey was conducted on November 3, 1975, 7 hours after the beam was turned off. The highest loss point in the Switchyard is the shield at the upstream end of Enclosure C. This device limits the size of the beam entering the beam splitting (Lambertson) magnets. Other loss points in the Switchyard include the Lambertson magnets located in the upstream ends of Enclosures B and

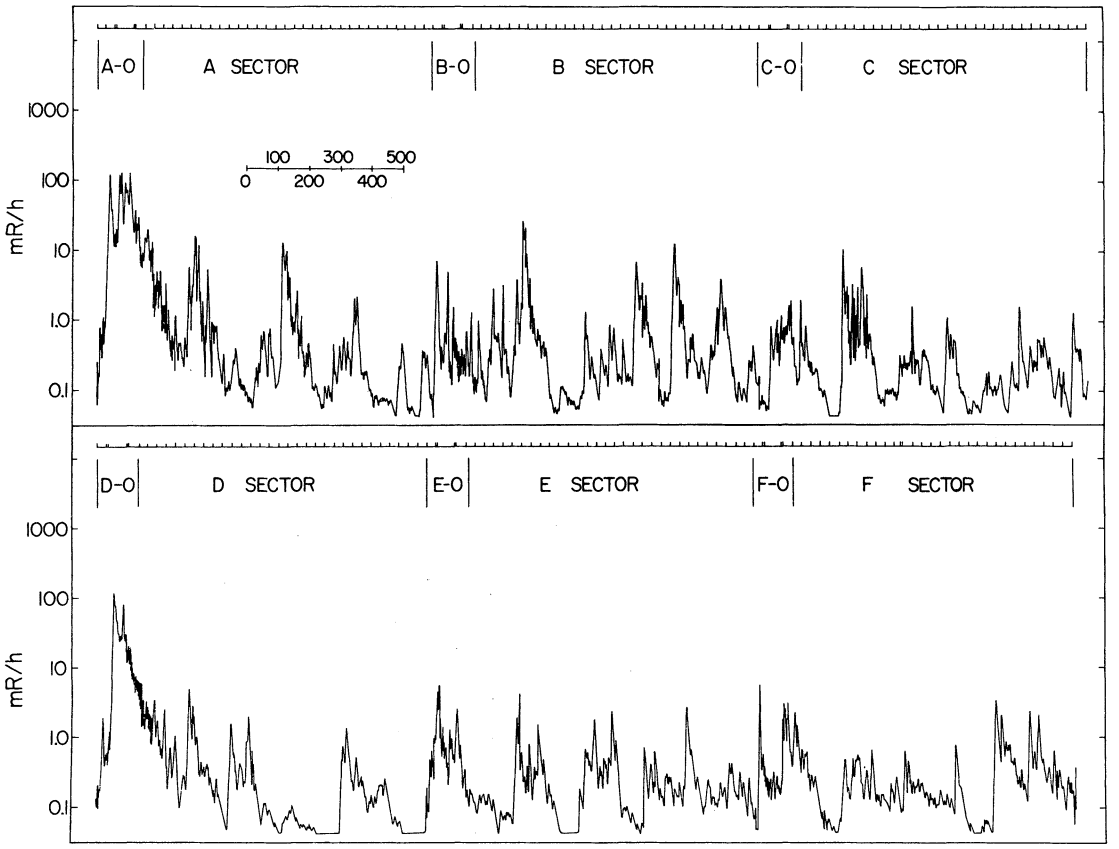

FIGURE 3 Radiation survey vehicle strip chart of the Fermilab Main Ring. The event marker at the top of the chart indicates the location of quadrupole magnets (~30 m apart) for horizontal axis calibration. This survey was made on October 16, 1975.

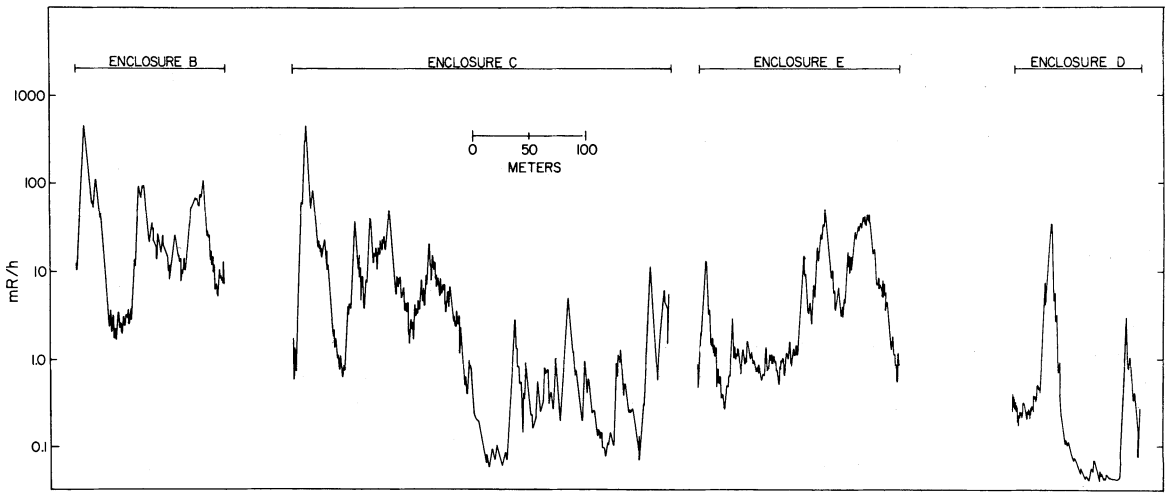

FIGURE 4 Radiation survey vehicle strip chart of the Fermilab Switchyard showing radiation intensity vs position on November 3, 1975.

C and the electrostatic septa in Enclosures B and E.

The scaler data permit the study of long-term changes in residual radioactivity throughout the accelerator. To make these data more meaningful, corrections are made to the scaler readings for the short-term decay in activity which takes place during the first few hours after the accelerator has been turned off. Figures 5, 6, and 7 show typical decays of residual radioactivity in the Booster, Main Ring, and Switchyard enclosures, respectively.

Figures 8 and 9 show the radiation intensity resulting from residual radioactivity in the Booster Accelerator as a function of time. Figure 8 contains plots of the radiation intensity, measured at a

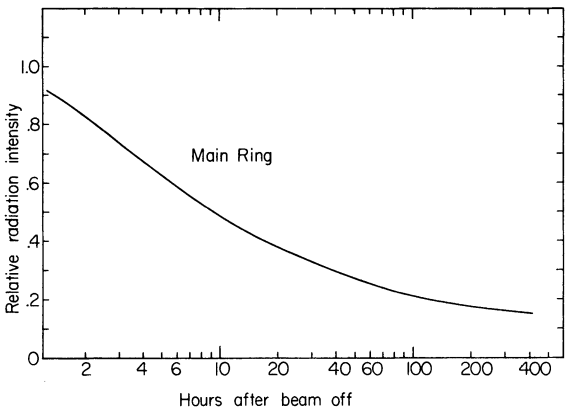

FIGURE 6 Radioactivity decay plot for the Main Ring showing relative radiation intensity vs hours after beam off.

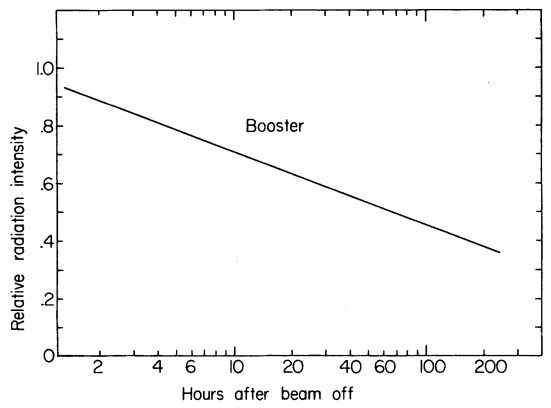

FIGURE 5 Radioactivity decay plot for the Booster accelerator showing relative radiation intensity vs hours after beam off.

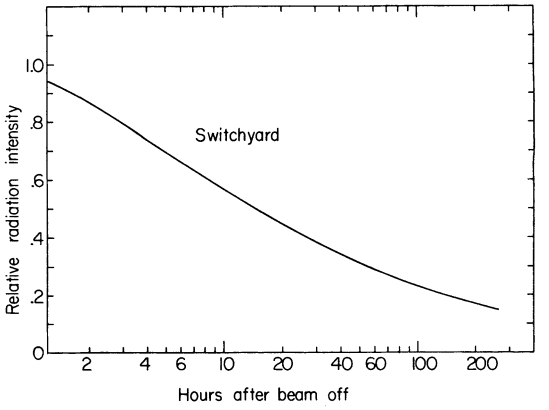

FIGURE 7 Radioactivity decay plot for the Switchyard showing relative radiation intensity vs hours after beam off.

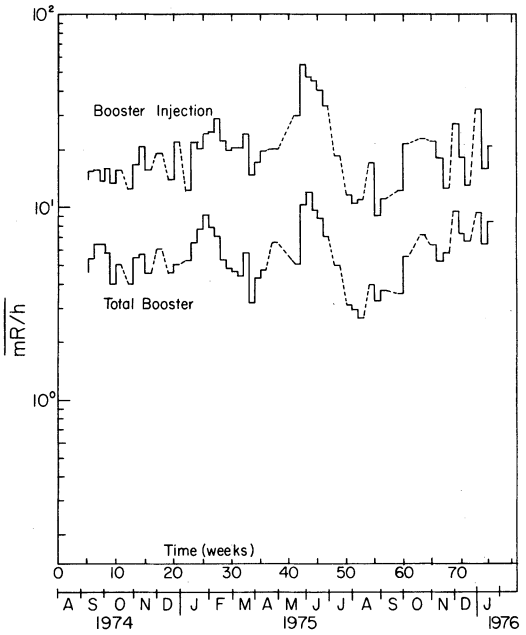

FIGURE 8 Mean radiation intensity vs time for the total Booster enclosure and for the 200-MeV proton injection segment of the Booster enclosure. For Figures 8 through 14 all intensities have been corrected to their value at 8 hours after beam off, and dashed lines indicate no surveys during these weeks.

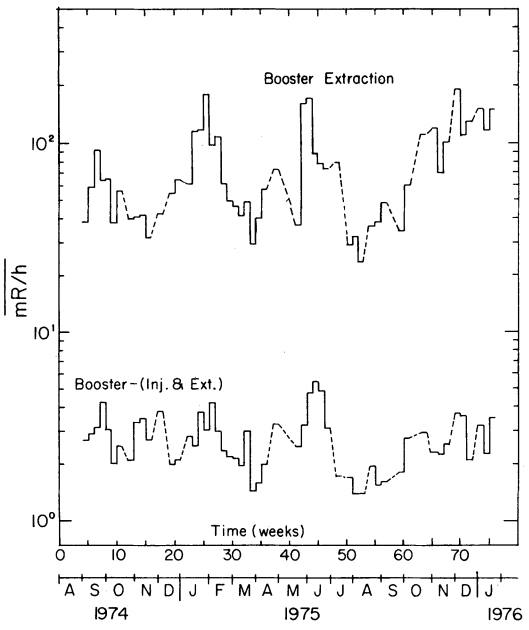

FIGURE 9 Mean radiation intensity vs time for the 8-GeV proton extraction segment of the Booster enclosure and for the total Booster less injection plus extraction.

distance of 30 cm from the Booster magnets, averaged over the injection segment and over the 471 m circumference of the accelerator. All radiation intensities have been corrected to indicate their value at eight hours after the beam was turned off. Figure 9 contains similar plots of data for the extraction segment of the Booster Ring and for the total Booster less injection and extraction. Figure 10 shows the radiation intensity (8 hours after beam-off) averaged over the 6.28 km circumference of the Fermilab Main Ring and over the 150-m-long Transfer Hall. Figure 11 contains a similar plot of radiation intensity for the Main Ring less the Transfer Hall and the beam abort segments. Figures 12, 13, and 14 show the mean radiation intensities in the Switchyard enclosures. Mean intensities were not measured in the Switchyard prior to January 1975.

Errors in the measurements shown in Figures 8–14 are estimated to be within $\pm 20\%$. This degree of accuracy is sufficient since the primary function of these data is to show long-term trends in residual radioactivity. Figure 15 is a graph of the total number of protons accelerated per week in the Main Ring as a function of time. Prior to July 1975, the Main Ring was operated at 300 GeV. 400-GeV operation was begun in late July 1975, and continues until the present writing. To some

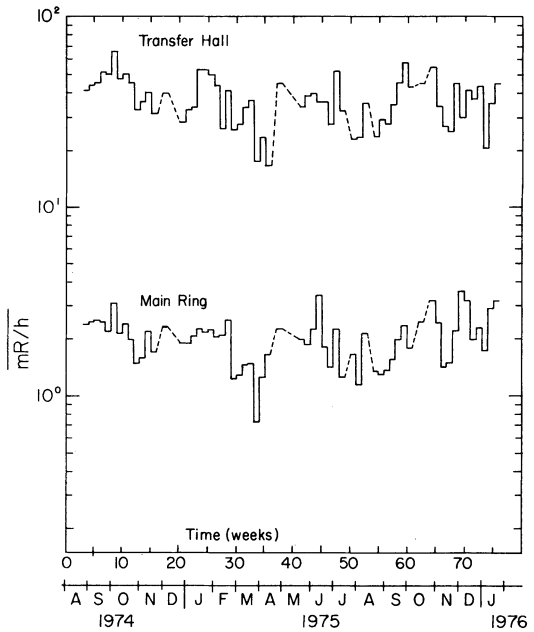

FIGURE 10 Radiation intensity vs time for the Fermilab Main Ring and for the Transfer Hall.

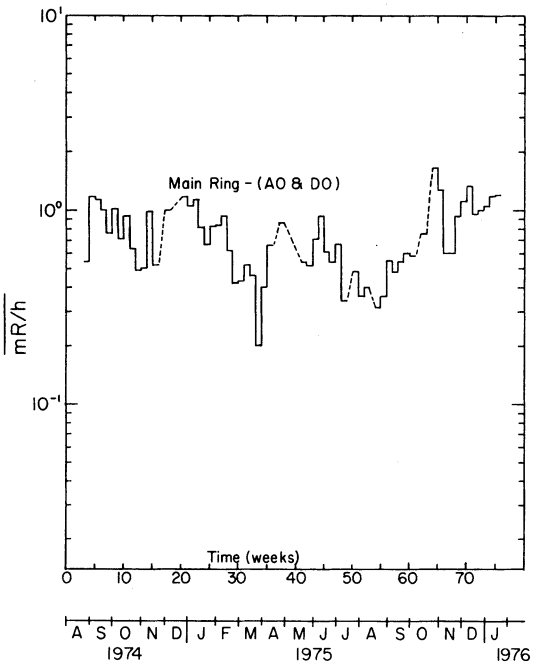

FIGURE 11 Mean radiation intensity vs time for the Main Ring less Transfer Hall and Beam Abort.

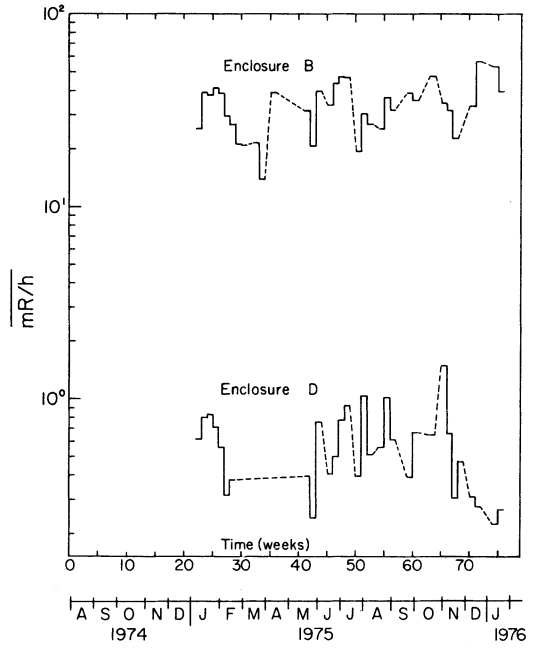

FIGURE 12 Mean radiation intensity vs time for the Switchyard Enclosures B and D.

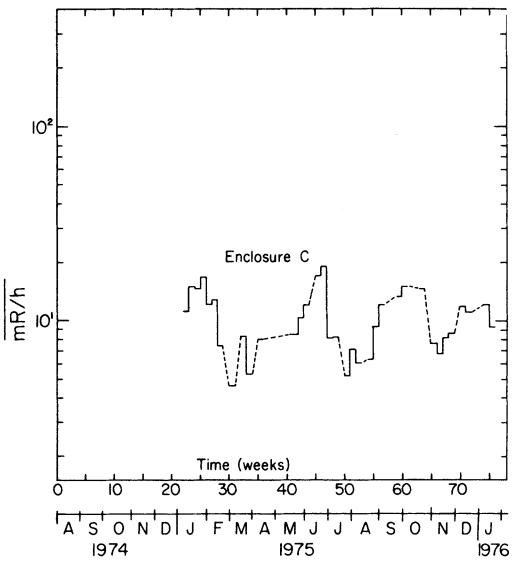

FIGURE 13 Mean radiation intensity vs time for the Switchyard Enclosure C.

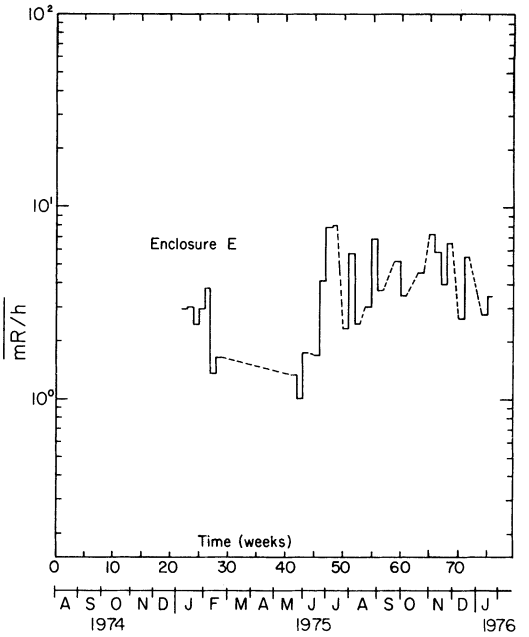

FIGURE 14 Mean radiation intensity vs time for the Switchyard Enclosure E.

extent the trends in Figure 15 are also present in the residual radioactivity graphs (Figures 8–14). It should be pointed out that during the Summer of 1975 several important changes were made in the alignment of hardware in the Booster injection region. These resulted in the pronounced peaks in the two curves of Figure 8.

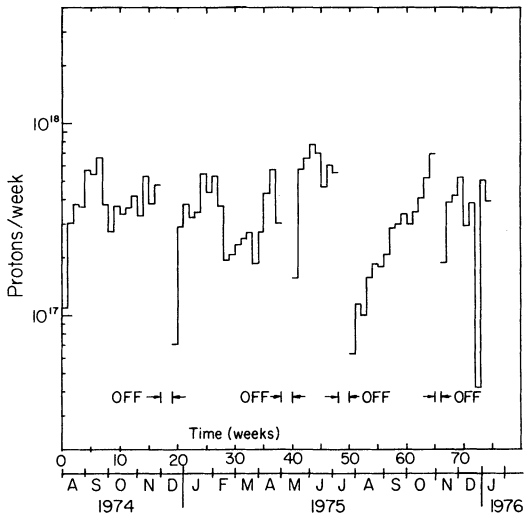

FIGURE 15 Main Ring beam intensity (protons/week) vs time. "Off" indicates periods when the accelerator systems were shut down for extended maintenance and development work.

CONCLUSIONS

Perhaps the most important feature of the data presented here is the stability of the residual radioactivity as a function of time. Effects which might influence the long-term residual radioactivity levels are beam-line losses, injection and extraction efficiency, proton energy, and proton beam intensity. The efficiency with which 8-GeV protons are injected and captured into the Main Ring is approximately 85% to 90% and is fairly stable in time. About 5% of the proton beam is lost at various points in the Main Ring during the three-second acceleration period. Main Ring extraction losses vary between 1% and 1.5%. The residual radioactivity present in the Main Ring enclosure is directly proportional to these losses.

It may be noted that the change in Main Ring operation from 300 GeV to 400 GeV in late July 1975 is not noticeable in any of these plots. It would, therefore, seem reasonable to predict that additional increases in proton energy would not result in marked increases in residual radioactivity. During August, September, and October 1975, there was a steady increase in beam intensity (Figure 15). A corresponding increase in residual radioactivity during this period is discernable in the graphs shown here, but the radioactivity increases at a much lower rate than the beam intensity, indicating that beam losses during this period rose more slowly than beam intensity.

In conclusion, it can be said that since August 1974, when measurements of mean radiation intensity began, the long-term trend in residual radioactivity has been rather stable in most parts of the Fermilab accelerator. Over periods of weeks, excursions related to accelerator output and efficiency have been noted, but most enclosures have nearly the same level of residual activity in late 1975, as they had in mid-1974. The long-term residual radioactivity data of the type presented here are important in predicting the conditions which will attend projected changes in accelerator configuration and operation. From the past history of residual radioactivity build-up as a function of known proton losses an estimate of future radiation levels within beam-line enclosures can be made, and safe working conditions and procedures in these areas can be established.

ACKNOWLEDGEMENTS

The authors wish to express their appreciation to Dr. D. D. Jovanovic for many helpful discussions and to J. C. Bauman for performing the computations involved in this work.

REFERENCES

1. R. R. Wilson, *Scientific American*, **230**, No. 2, 72 (1974).
2. R. E. Shafer and D. D. Jovanovic, *IEEE Trans. Nuc. Sci.*, **NS-20**, No. 3, 499 (1973).